sustainability

MDPI

Article

Quantifying the Morphological Evolution of Shallow-Water Lakes Using a Volume Change Model: A Case Study of Poyang Lake

Yang Li [1], Yeyang Xie [1], Lansong Lv [2], Juan Fu [2], Junkai Zhao [3], Zijun Li [1,*] and Shuwei Zheng [1,4,*]

[1] School of Geography and Environment, Shandong Normal University, Jinan 250358, China
[2] Shandong Provincial Territorial Spatial Ecological Restoration Center, Jinan 250110, China
[3] College of Tourism and Geography, Jiujiang University, Jiujiang 332005, China
[4] Coastal Studies Institute, Louisiana State University, Baton Rouge, LA 70803, USA
* Correspondence: lizijun@sdnu.edu.cn (Z.L.); 618067@sdnu.edu.cn (S.Z.)

Abstract

Reliable quantification of morphological evolution in shallow-water lakes constitutes a long-standing challenge for limnological studies, which is essential to advance sustainable lake-basin management. Poyang Lake is a typical shallow-water lake, featuring a basin composed of narrow channels and extensive shallow bottomlands. This geomorphological feature leads to a variety of eco-environmental problems. Using the Google Earth Engine (GEE) platform and field-measured water level data, this study constructed a volume change model (VCM) to estimate changes in water storage (volume) across water levels ranging from 8 m to 14 m in Poyang Lake during 1989–2025. In the VCM, annual surface water areas at the two characteristic water levels (8 m and 14 m, approximating the 25th and 75th percentiles of the long-term water-level record) were first derived. Thus, the volume changes reflect lake-basin morphological change rather than hydrological variability. The results show that lake volume (8–14 m) decreased by 2515.5 $\times$ 10^4 m^3 over 1989–2025, an equivalent of 3018.6 $\times$ 10^4 t sediment for the lake basin material. Specifically, the lake basin experienced deposition (1092.0 $\times$ 10^4 t), erosion (2052.0 $\times$ 10^4 t) and deposition (3984.0 $\times$ 10^4 t) during 1989–1999, 1999–2007 and 2007–2025, respectively. The volume change model can effectively quantify lake volume change. Intense basin-wide precipitation led to net sediment deposition during 1989–1999, while large-scale unregulated sand mining operations were closely associated with an increase in the lake volume in 1999–2007. Since 2007, enforced sand-mining regulations have greatly reduced in-lake sand extraction. The sediment input change and sand-mining regulations lead to net sediment accumulation across the Poyang Lake basin.

Keywords: lake morphological evolution; water storage change; sand mining; Google Earth Engine; Poyang Lake

Check for updates

Academic Editor: Antonio Miguel Martínez-Graña

Received: 1 September 2026
Revised: 14 October 2026
Accepted: 24 October 2026
Published: 29 October 2026

Copyright: © 2026 by the authors. Licensee MDPI, Basel, Switzerland. This article is an open access article distributed under the terms and conditions of the Creative Commons Attribution (CC BY) license.

1. Introduction

As natural water bodies widely distributed in the terrestrial surface system, lakes cover approximately 3% of the global land area [1,2]. They play an irreplaceable role in water supply, biodiversity conservation, and regional sustainable development [3], while also serving as a critical link in biogeochemical processes [4]. Freshwater lakes, in particular, constitute a vital foundation for the sustainable development of human society. Possessing ecological service

functions such as drinking water supply, agricultural irrigation, and flood regulation and storage, they act as important barriers for regional water and ecological security [5,6]. Although the natural evolution of lake morphology is typically slow and continuous, contemporary shallow-water lake morphology is undergoing rapid and complex transformations driven by the combined effects of global climate change and intensive human activities [7,8]. Here, shallow-water lakes are commonly defined as lakes whose mean depth is small relative to their surface area; lacking persistent thermal stratification, they are frequently mixed down to the bed, so that basin morphology, hydrodynamics and ecological processes are tightly coupled [8]. Consequently, shallow-water lake morphological evolution, its underlying driving mechanisms, and ecological effects have emerged as one of the core topics in limnological science and regional sustainable-development research.

Water storage capacity is one of the key indicators characterizing the eco-hydrological functions and health status of lakes [1]. Changes in lake water storage are jointly regulated by multiple factors, including changes in lake basin morphology, inflow recharge, climate change, and anthropogenic activities [9,10]. Based on an analysis of Landsat satellite imagery for 1972 global lakes over the past three decades, Yao et al. [1] revealed that approximately 53% of lakes worldwide exhibited a declining trend in water storage between 1992 and 2020. Zhao et al. [11] indicated that intensified water evaporation may also be a significant factor contributing to the decline in lake water storage. Conversely, the study of Barnett and Pierce [12] on Lake Mead found that reduced watershed inflow is the primary factor causing the continuous decline of the lake's water storage. Furthermore, climate change has also profoundly influenced the global patterns of lake water storage by altering processes such as precipitation and evaporation [13]. Notably, disturbed by intensive anthropogenic activities, lake basin morphology can undergo drastic changes over short periods; for instance, large-scale sand mining activities significantly alter lake morphology, thereby leading to changes in water storage [14,15]. Currently, relevant studies predominantly focus on the impacts of lake water budgets and climate change on water storage changes [9,16,17]. However, the impact of rapid changes in shallow-water lake morphology on water storage remains less systematically understood. Moreover, this limitation hinders an in-depth understanding of the evolutionary mechanisms of shallow-water lake water storage on decadal scales. In particular, although remote-sensing and GEE-based approaches have been widely used to monitor the water area and storage of lakes [18–21] and to infer their bathymetric and hydrological changes [22,23], works that convert area changes at fixed water levels directly into basin-volume and sediment-mass changes are still lacking.

Poyang Lake is a typical freshwater shallow-water lake, with a lake basin consisting of narrow channels and extensive bottomlands. Its drainage basin covers an area of approximately 16.22×10^4 km^2, accounting for 1.69% of China's total land area [24]. With distinct water level changes between the flood and dry seasons, it is a typical flow-through, river-connected lake [25,26]. Previous studies indicate that the water surface area of Poyang Lake can reach 2800.79 km^2 during the flood season, whereas it shrinks to 1242.03 km^2 in the dry season [24,27]. The flood-season area is 3 to 4 times that of the dry season, resulting in corresponding changes in lake water storage. However, in recent years, Poyang Lake has experienced an earlier onset of the dry season and the normalization of low water levels, leading to significant declines in water surface area and lake storage. Consequently, regional water-resource sustainability is confronted with severe challenges [27,28], including insecure water supply for surrounding cities, degradation of wetland habitats for migratory birds, and weakened flood regulation and storage capacity. In contrast, Mei et al. [27] argue that the regulation of the Yangtze River by the Three Gorges Dam significantly affects the water levels and water storage of Poyang Lake. Meanwhile, high-intensity sand mining

activities in the lake basin may also induce significant morphological changes in certain areas [16]. However, further studies have pointed out that the erosion and deposition evolution within the Poyang Lake basin exhibits spatial heterogeneity [29,30]. Therefore, scientifically assessing the morphological evolution of Poyang Lake is not only a currently urgent scientific problem, but also of great practical significance for water resource management, flood and drought control, wetland ecosystem conservation, and regional sustainable development [31–33].

Overall, based on the Google Earth Engine platform and in situ hydrological data from the Poyang Lake basin, this study focuses on: (1) constructing a lake volume change model (VCM) based on multi-source remote sensing data and field-measured water level data, and (2) quantitatively assessing morphological changes in the Poyang Lake basin across characteristic water level ranges. The findings of this study are expected to deepen insights into the evolutionary processes of shallow-water lakes, while offering scientific support for sustainable development and utilization of shallow-water lakes around the world. This work builds on established hypsographic and storage-curve approaches [9,18,19] and extends them by directly converting area changes at fixed water levels into sediment-mass changes, thereby addressing the long-standing challenge of quantifying shallow-lake morphological evolution in the absence of bathymetric surveys.

2. Materials and Methods

2.1. Study Area

Poyang Lake (28°22′~29°45′ N, 115°47′~116°45′ E, Figure 1) is located in northern Jiangxi Province, on the southern bank of the middle Yangtze River, at the junction of Jiujiang, Nanchang, and Shangrao cities. It receives water from the five major river systems, Ganjiang River, Fuhe River, Xinjiang River, Raohe River, and Xiuhe River, making it a typical water-carrying, inflow–outflow seasonal shallow-water lake [34]. These five tributaries account for 85.4% of the total runoff and 87.2% of the suspended sediment load entering Poyang Lake [35]. As the largest freshwater lake in China, Poyang Lake possesses a complete river system and abundant water resources, with a multi-year average runoff of 1525×10^8 m^3. It stretches 170 km from north to south and 74 km from east to west [27]. Covering a total drainage area of 16.22×10^4 km^2, the basin accounts for 1.69% of China's total land area and 9% of the entire Yangtze River Basin, playing a pivotal role in the patterns of water and ecological security within the Yangtze River Basin [24]. The Poyang Lake basin is characterized by a subtropical monsoon climate, with an annual precipitation of 1654 mm and a mean annual temperature of 17.6 °C [36].

Since 2000, driven by sand mining control policies in the main stem of the Yangtze River, large-scale sand mining operations have gradually shifted to the Poyang Lake basin and its tributaries [37]. This intensive sand mining activity has directly induced drastic alterations to both the lake basin morphology of Poyang Lake and the geomorphology of its connecting channel to the Yangtze River [16,38]. Concurrently, the continuous implementation of soil and water conservation projects and ecological protection policies in the upper basin has profoundly altered sediment transport and deposition processes in Poyang Lake, leading to significant changes in its hydrological regimes [7,36]. Phenomena such as the earlier onset of the dry season and the normalization of low water levels in Poyang Lake have become increasingly pronounced [39,40]. Against the backdrop of continuous changes in hydrological regime and lake morphology, the stability of the wetland ecosystem, the integrity of aquatic habitats, and the regional flood regulation and storage functions all face severe challenges [25,29].

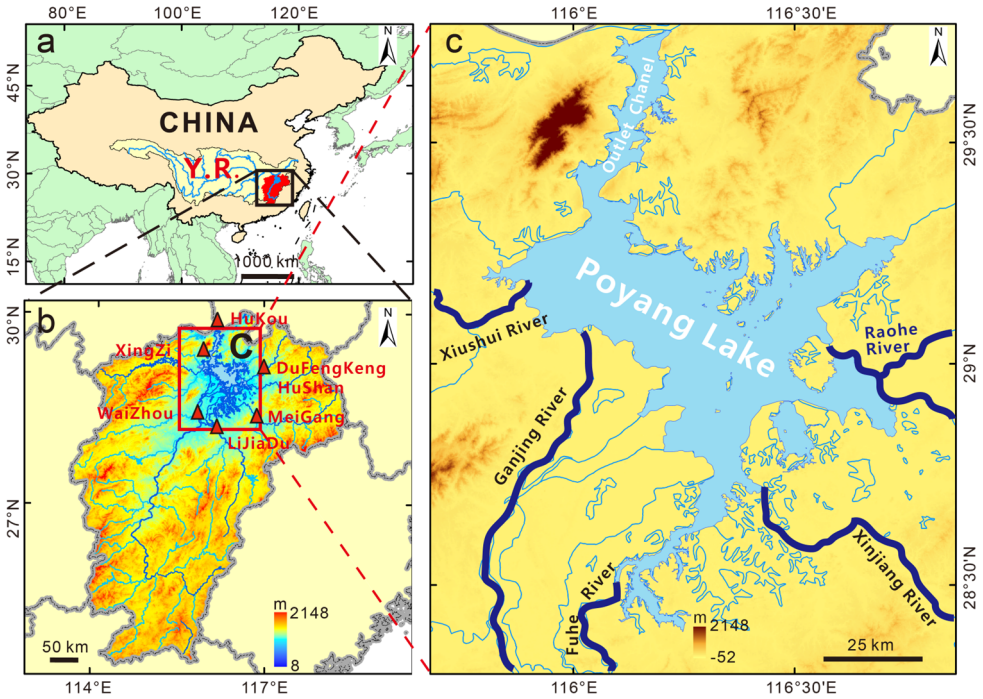


Figure 1. Maps of the study area. (**a**) Map shows the location of the Yangtze River (Y. R.). (**b**) Map shows the location of Poyang Lake basin and hydrologic stations. Red triangles indicate the locations of hydrological stations. (**c**) Map shows the outlet channel and the tributary estuaries.

2.2. Data Sources

Annual runoff and sediment discharge data for Poyang Lake from 1989 to 2025 were obtained from the Changjiang Water Resources Commission of the Ministry of Water Resources (accessed on 4 June 2026, http://www.cjw.gov.cn/) [41]. Specifically, data for the Gan River were derived from the Waizhou station, the Fu River from the Lijiadu station, the Xin River from the Meigang station, the Rao River from the Hushan station, and the Xiu River from the Wanjiabu station. Furthermore, the Hukou station data were adopted as the outflow hydrological data for Poyang Lake (accessed on 4 June 2026, http://www.cjw.gov.cn/) [41]. Additionally, water levels within the Poyang Lake area were represented by data from the Xingzi station [41].

Based on the Google Earth Engine (GEE, https://code.earthengine.google.com (accessed on 22 July 2025) platform, cloud cover and image extent were used to screen the Landsat series data from 1989 to 2025. A total of 378 remote sensing images meeting the criteria were selected from an initial pool of 660 images. Specifically, 228 images were from Landsat-5 TM (spanning 1989–2011), 116 from Landsat-8 OLI/TIRS (spanning 2013–2025), and 34 from Landsat-9 OLI-2/TIRS-2 (spanning 2021–2025) (Table 1). Landsat-7 ETM+ imagery was not used because the scan-line-corrector failure after 2003 leaves data gaps of about 22% in each scene, which would introduce systematic bias into area estimation; the available Landsat-5/8/9 images already provide adequate temporal coverage.

Table 1. Landsat satellite data used in the study.

Satellite	Bands	Resolution	Acquisition Time	Number
Landsat-5	SR_B2(Green) SR_B5(SWIR)	30 m	1989–2011	228
Landsat-8	SR_B3(Green) SR_B6(SWIR)		2013–2025	116
Landsat-9			2021–2025	34

2.3. Methods

2.3.1. Division of Study Periods

Unregulated sand mining in the main stream of the Yangtze River once triggered a series of ecological and environmental problems. In 2000, the General Office of the State Council forwarded the Notice on Opinions for Strengthening Sand Mining Administration in the Middle and Lower Reaches of the Yangtze River issued by the Ministry of Water Resources, explicitly prohibiting illegal sand mining in these river reaches [42]. Subsequently, a large number of sand mining vessels moved their operations to Poyang Lake [43]. To address the disorder caused by unregulated sand mining in Poyang Lake, the Jiangxi Provincial People's Government forwarded the Opinions on Further Strengthening Sand Mining Management in the Middle and Lower Reaches of the Gan River and Poyang Lake, issued by the Provincial Department of Water Resources in 2008. In 2016, the Regulations on River Channel Sand Mining Management in Jiangxi Province were officially promulgated [44], marking the transition of sand mining in Poyang Lake into a phase of scientific regulation. Based on these critical policy milestones, this study divides the research period into three stages: (1) the small-scale mining stage (1989–1999); (2) the large-scale unregulated mining stage (2000–2007); (3) the comprehensive regulation and scientific management stage (2007–2025). It is worth noting that the year 2007 was chosen as the boundary between the second and third stages because the 2008 provincial regulation effectively ended the large-scale unregulated mining that had peaked during 2000–2007. However, the 2016 provincial regulations marked a further deepening of scientific management within the third stage rather than the start of a separate stage.

2.3.2. Surface Water Area Extraction Methods

In this study, the Modified Normalized Difference Water Index (MNDWI) [45] was employed to extract the water area of Poyang Lake. Compared with the Normalized Difference Water Index (NDWI), MNDWI substitutes the near-infrared band with the mid-infrared band. This allows for the effective separation of water bodies from background information such as vegetation and buildings, enabling the precise extraction of various water types, including the main lake area, the channel into the Yangtze River, and the saucer-shaped lakes. The calculation formula is as follows:

$$MNDWI = \frac{Green - MIR}{Green + MIR} \quad (1)$$

In this equation, Green is the green band of the Landsat image, and MIR refers to the mid-infrared band.

To reduce subjective errors caused by manual threshold selection, this study employed the Otsu algorithm to perform automatic threshold segmentation on MNDWI images. The Otsu algorithm is an adaptive threshold segmentation method based on the image grayscale histogram. Its core principle involves identifying an optimal threshold to maximize the between-class variance of the foreground (water) and the background (non-water), thereby achieving precise separation between water and non-water areas [46]. Let the gray level probability of an image be pi, and the probabilities and mean gray values of the foreground and background be ω0, ω1 and μ0, μ1 respectively. Then the between-class variance is defined as:

$$\sigma_b^2(T) = \omega_0(T)\omega_1(T)[\mu_0(T) - \mu_1(T)]^2 \quad (2)$$

The optimal threshold T* is determined by maximizing the inter-class variance (Otsu's method) [46].

$$T^* = \arg[\max_{0<T<L-1} \sigma_b^2(T)] \quad (3)$$

The Otsu algorithm requires no manual threshold selection, is computationally simple, and exhibits strong robustness; thus, it is widely used in remote sensing water extraction [17,47]. Combining this algorithm with water indices (e.g., NDWI, MNDWI) enables the automatic and precise separation of water and non-water areas, significantly improving the segmentation accuracy of remote sensing images.

2.3.3. Accuracy Assessment of Surface Water Area Extraction Methods

To evaluate the accuracy of surface water area extraction based on the Google Earth Engine (GEE) platform, this study randomly selected remote sensing images of Poyang Lake from a specific period. Surface water area extraction was performed simultaneously using the GEE platform and visual interpretation (ENVI 5.6 software), followed by a comparative analysis of the results from the two methods. The main workflow of visual interpretation includes image preprocessing, selection of interpretation objects, visual interpretation and analysis, feature type labeling, and statistical data compilation. The following formula was adopted to quantitatively assess the accuracy of the surface water area extracted via the GEE platform:

$$\mathcal{E} = a/b \quad (4)$$

In this study, the surface water area extracted via visual interpretation (denoted as a) served as the accuracy benchmark, while the surface water area of Poyang Lake extracted based on the GEE platform (denoted as b) acted as the subject of accuracy evaluation (Figure 2). $\mathcal{E}$ is the ratio; a value closer to 1 indicates that the GEE-derived data more closely align with the visual interpretation results, signifying better accuracy.

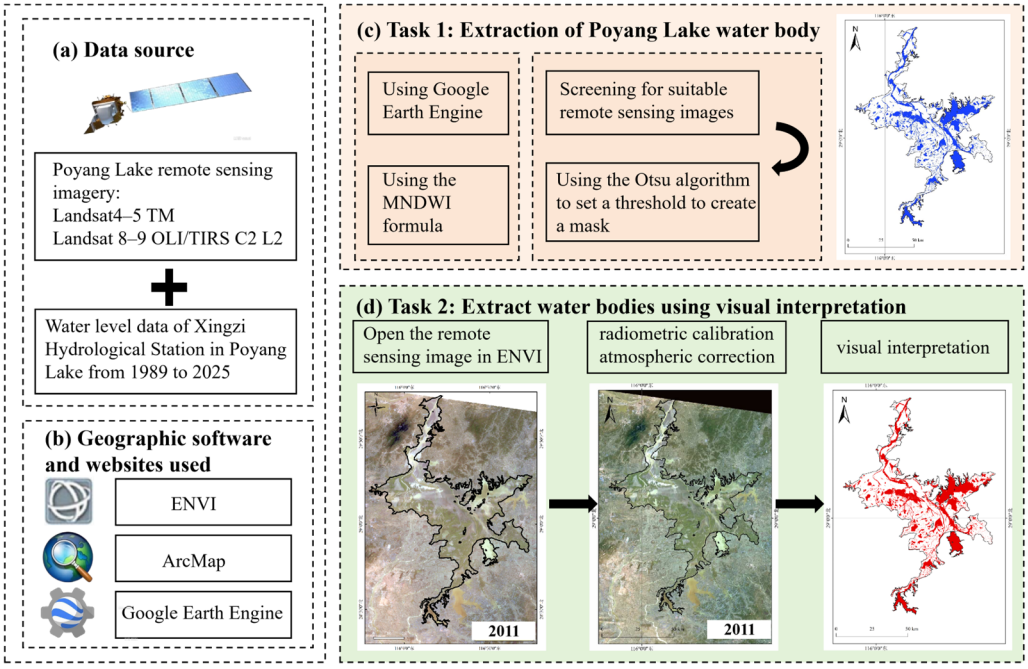


Figure 2. GEE technology roadmap for water extraction. The blue area denotes the water body to be extracted (**c**). The red area denotes the extracted water body (**d**). Black arrows show the direction of workflow steps.

2.3.4. Selection of Characteristic Water Levels in Poyang Lake

Considering the significant amplitude of water level fluctuations between flood and dry seasons in the Poyang Lake area (ranging from 5.11 to 20.65 m) and the uneven spatial distribution of water levels (e.g., the water levels corresponding to the 75th and 25th percentiles are approximately 14 m and 8 m, respectively; Figure 3a), as well as the fixed revisit cycle of

remote sensing imagery and the susceptibility of data quality to cloud cover interference, this study incorporated water level monitoring data to conduct a detailed review and screening of annual remote sensing imagery from 1989 to 2025. Ultimately, the number of images available for analysis in each study period was determined as follows: 84 images from 9 years were selected for 1989–1999 (Figure 3b), 96 images from 8 years for 2000–2007 (Figure 3c), 88 images from 8 years for 2008–2015 (Figure 3d), and 110 images from 7 years for 2016–2025 (Figure 3e). The selected images are distributed across different months and hydrological seasons within each year (Figure 3b–e), covering flood and dry seasons as well as rising and falling water-level limbs. The annual water level–area fits therefore represent typical basin morphology rather than seasonally skewed hydrological states. Owing to cloud contamination and image availability, 32 of the 37 years between 1989 and 2025 have usable images. Landsat-7 ETM+ was excluded because the scan-line-corrector failure after 2003 leaves data gaps of about 22% per scene.

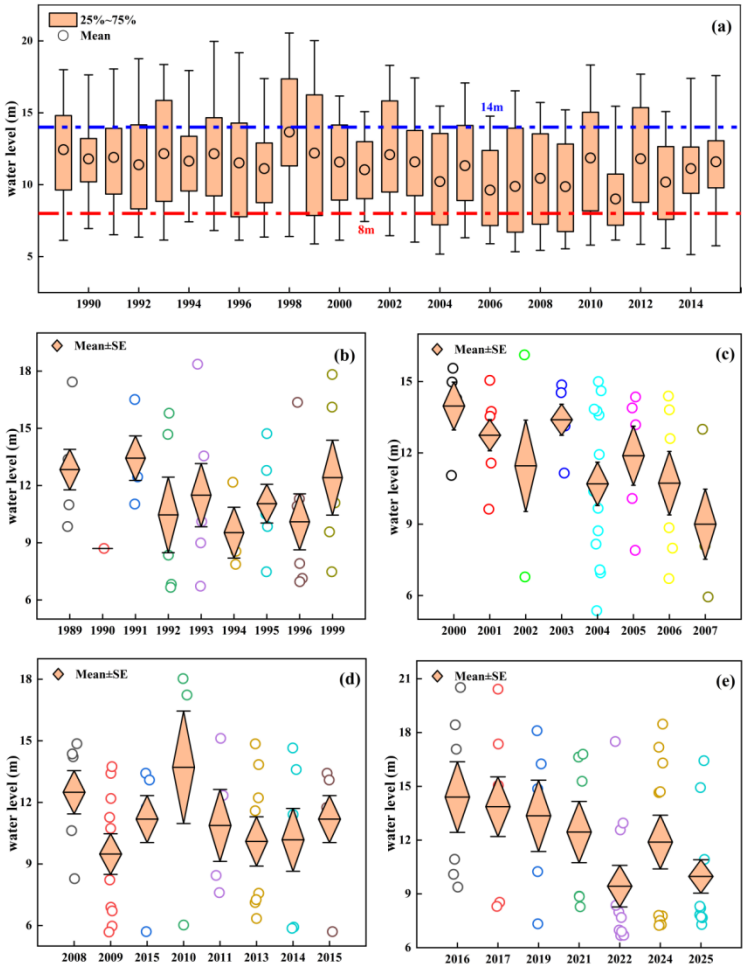


Figure 3. (**a**) Distribution of daily water levels at Xingzi Station during 1989–2025; (**b**–**e**) water levels corresponding to the selected remote-sensing images during 1989–1999 (**b**), 2000–2007 (**c**), 2008–2015 (**d**) and 2016–2025 (**e**).

2.3.5. Estimation of Surface Water Area

Analysis combining remote sensing imagery and water level monitoring data reveals that there are differences in lake water levels corresponding to the acquisition times of remote sensing imagery across different years. This leads to a lack of direct comparability in the annual surface water area data of Poyang Lake. Therefore, it is necessary to correct the historical surface water areas to a unified water level condition before conducting time-series comparative analysis. This study employed a quadratic polynomial fitting

method to fit the water level and surface water area data within the same year, thereby calculating the surface water area corresponding to a characteristic water level (Figure 4a). The quadratic polynomial used for fitting is as follows:

$$S = aH^2 + bH + c \quad (5)$$

where S is the surface water area (m^2), H is the water level (m) and a, b, and c are the model parameters to be fitted.

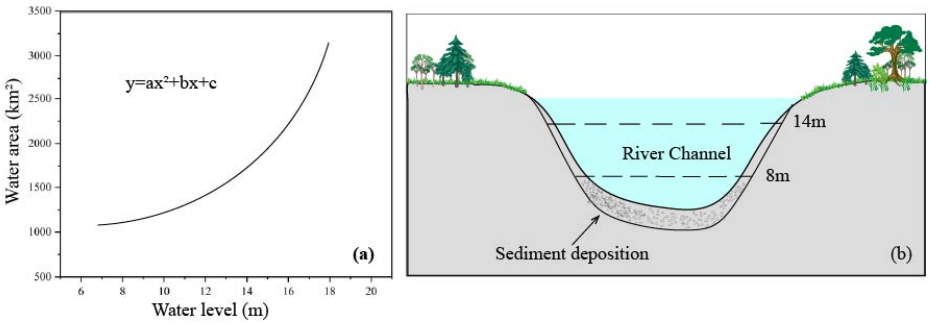


Figure 4. (**a**) Surface water area–water level relationship fitted by the quadratic polynomial (Equation (5)); (**b**) lake volume change and water levels.

To evaluate the fitting performance of the quadratic polynomial, the Standard Error of Estimate (SEE) was adopted for accuracy assessment. The calculation formula for SEE is:

$$SEE = \sqrt{\frac{\sum_{i=1}^{n}\left(S_i - \hat{S}_i\right)^2}{n - p}} \quad (6)$$

where is the extracted surface water area, is the model predicted area, is the sample size, and is the number of model parameters. Meanwhile, the relative SEE is calculated, with S representing the average extracted water area:

$$SEE_{rel} = \frac{SEE}{\bar{S}} \times 100\% \quad (7)$$

2.3.6. Develop the Volume Change Model (VCM)

As mentioned previously, considering the impact of water level conditions and the quantity of imagery on fitting results, this study focuses on estimating the surface water area of Poyang Lake corresponding to the 75th percentile (approx. 14 m) and the 25th percentile (approx. 8 m). Thus, the 8–14 m water level interval was taken as the characteristic water level range in this study. It should be clarified that the water volume change in this study does not denote the total volume change of the entire lake, but specifically refers to the water volume change within the 8–14 m water level range. Two points should be emphasized. First, because the surface areas used in Equations (8)–(10) are estimated at fixed water levels (8 m and 14 m), hydrological variability—inter-annual differences in inflow, outflow and evaporation—is normalized out. Thus, at a given water level, the water surface area is determined by basin morphology, so the volume change ΔV of the 8–14 m layer between two years reflects net sediment deposition or erosion rather than hydrological fluctuation. Second, Equations (8)–(10) apply the classical prismoidal (frustum) formula long used in reservoir surveying (Figure 5), so the geometric approximation error is small relative to the area-extraction and fitting uncertainties.

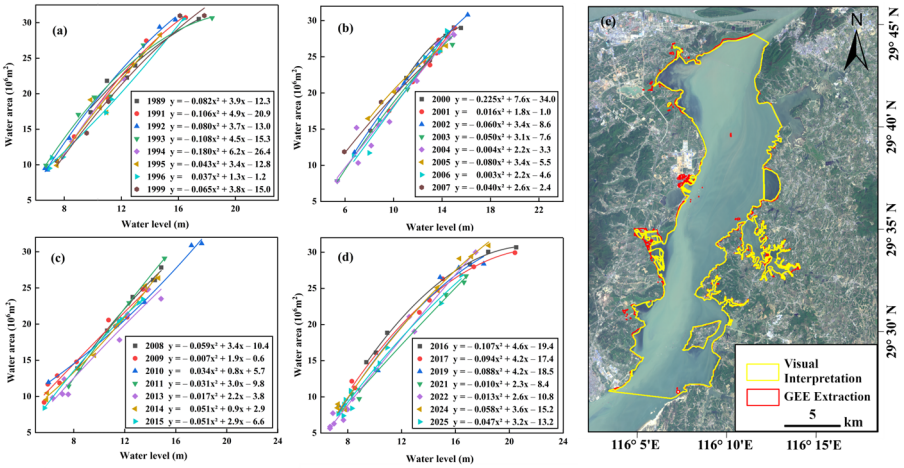


Figure 5. (**a**–**c**) Fitted surface water area–water level relationships at the 8 m and 14 m levels for 1989–1999 (**a**), 2000–2007 (**b**), 2008–2015 (**c**) and 2016–2025 (**d**); (**e**) comparison between the GEE-derived and visually interpreted water extraction maps (scene of 15 April 2020).

The surface water volume of Poyang Lake is calculated as follows:
The approximate volume for the 8–14 m range in year i:

$$V_i = \frac{1}{3} \cdot h \cdot \left(S_8^i + S_{14}^i + \sqrt{S_8^i \cdot S_{14}^i} \right) \quad (8)$$

The approximate volume for the 8–14 m range in year i+n:

$$V_{i+n} = \frac{1}{3} \cdot h \cdot \left(S_8^{i+n} + S_{14}^{i+n} + \sqrt{S_8^{i+n} \cdot S_{14}^{i+n}} \right) \quad (9)$$

The approximate volume change for the 8–14 m range between year i and year i + n:

$$\Delta V = V_{i+n} - V_i \quad (10)$$

where represents the surface water area at the 8 m water level in year i; represents the surface water area at the 14 m water level in year i; and ΔV is the volume change between the 8 m and 14 m water levels.

The sediment mass change (M) is calculated from the volume change (ΔV) of the channel–shoal system in each period using the following formula:

$$M = \rho \times \Delta V \quad (11)$$

In this equation, ρ is the bulk density of the sediment, which is taken as 1.2 t/m^3 [48] in this study.

3. Results and Analyses

3.1. Reliability Analysis of Water Area Estimation Results

A reliable fit of the surface water area-water level curve is a prerequisite for accurately analyzing changes in Poyang Lake's surface water volume. In this study, quadratic polynomial fitting was applied to the surface water area–water level curves of Poyang Lake from 1989 to 2025. The coefficients of determination (R^2) were all greater than 0.94, and the relative Standard Errors of Estimate (SEE) were all below 10%, indicating an excellent fitting performance (Figure 5a–c). Additionally, a remote sensing image acquired on 15 April 2020 (LC81210402020106LGN00) was randomly selected. A partial area of this image was subjected to visual interpretation (Figure 5d), and the results were compared

and validated against the surface water area extracted via the GEE platform. The results showed that the visually interpreted surface water area was 219.48 × 10^6 m^2, while the GEE-extracted area was 227.26 × 10^6 m^2, yielding an error of ±3.54%. This demonstrates the high reliability of the surface water area estimation results in this study. The images used for fitting span different months and hydrological seasons (Section 2.3.4), so the fitted water level–area relationships represent typical basin morphology rather than seasonally skewed conditions.

3.2. Change Characteristics of Surface Water Area

From 1989 to 2025, the surface water area of Poyang Lake corresponding to the 8 m water level exhibited a generally fluctuating downward trend, decreasing from 1350.8 × 10^6 m^2 in 1989 to 925.1 × 10^6 m^2 in 2025 (Figure 6). Specifically, from 1989 to 1999, the surface water area decreased from 1350.8 × 10^6 m^2 to 1128.8 × 10^6 m^2, with an average annual decrease of 22.2 × 10^6 m^2. From 1999 to 2007, the area rebounded sharply during 1999–2000 and then declined gradually, with the 2007 value (1582.0 × 10^6 m^2) still higher than that in 1999 (1128.8 × 10^6 m^2). From 2007 to 2025, the surface water area presented a downward trend again, dropping from 1582.0 × 10^6 m^2 to 925.1 × 10^6 m^2, with an average annual decrease of 36.5 × 10^6 m^2.

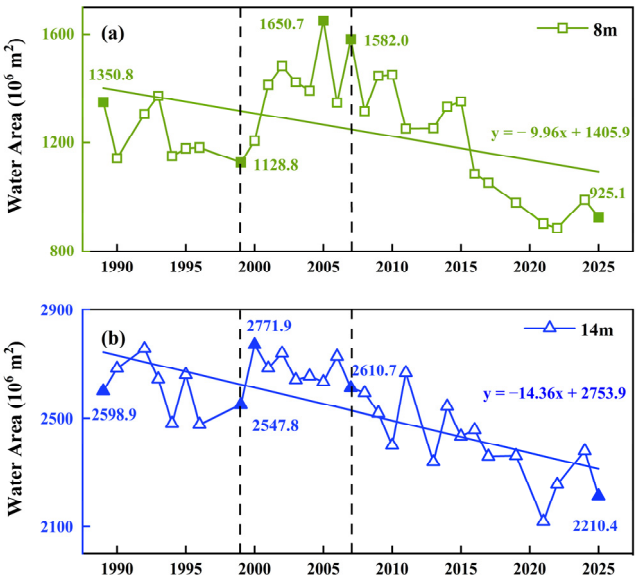


Figure 6. Change in surface water area: (**a**) under 8 m water level; (**b**) under 14 m water level. Green boxes and blue triangles represent water area data for 8 m and 14 m, respectively. Among them, solid symbols denote data with value labels.

Similarly, between 1989 and 2025, the surface water area corresponding to the 14 m water level also generally exhibited a fluctuating downward trend, declining from 2598.9 × 10^6 m^2 in 1989 to 2210.4 × 10^6 m^2 in 2025 (Figure 6). Specifically, from 1989 to 1999, the surface water area slowly decreased from 2598.9 × 10^6 m^2 to 2547.8 × 10^6 m^2, with an average annual decrease of 5.1 × 10^6 m^2. From 1999 to 2007, the area showed a slight net increase from 2547.8 × 10^6 m^2 to 2610.7 × 10^6 m^2, which occurred mainly around 1999–2000. From 2007 to 2025, the surface water area continued to decline, decreasing from 2610.7 × 10^6 m^2 to 2210.4 × 10^6 m^2, with an average annual decrease of 22.2 × 10^6 m^2.

3.3. Estimation of Volume Changes

3.3.1. Lake Volume Change Characteristics at 8–14 m

From 1989 to 2025, the basin volume of Poyang Lake within the 8–14 m water level range generally exhibited a fluctuating downward trend, decreasing from 116.5 × 10^6 m^3 in 1989 to 91.3 × 10^6 m^3 in 2025 (Figure 7). Specifically, from 1989 to 1999, the basin volume decreased from 116.5 × 10^6 m^3 to 107.4 × 10^6 m^3, with an average annual decrease of 90.2 × 10^4 m^3. From 1999 to 2007, the basin volume showed a significant recovery trend, increasing from 107.4 × 10^6 m^3 to 124.5 × 10^6 m^3, with an average annual increase of 213.1 × 10^4 m^3. However, from 2007 to 2025, the basin volume presented a rapid downward trend, dropping from 124.5 × 10^6 m^3 to 91.3 × 10^6 m^3, with an average annual decrease of 184.4 × 10^4 m^3; this rate of decline was significantly higher than that of the previous two periods.

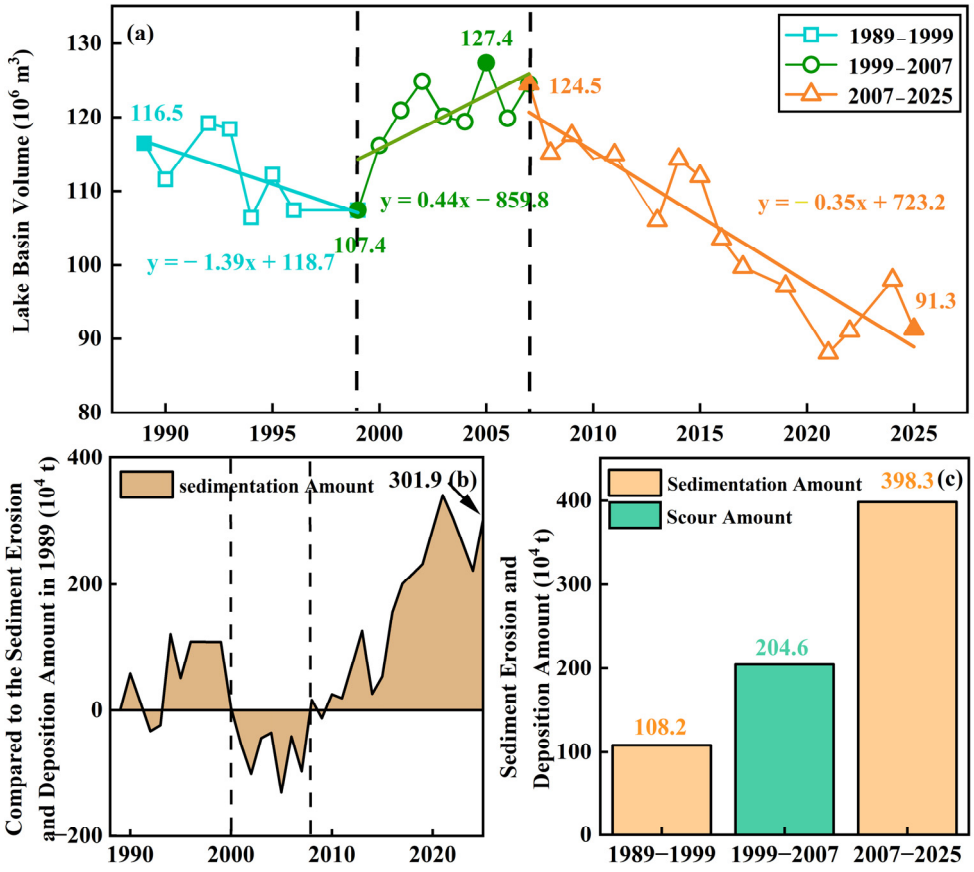


Figure 7. Changes in the basin volume of Poyang Lake at water levels of 8–14 m (**a**); Changes in sediment erosion and deposition relative to 1989 (**b**); Changes in sediment erosion and deposition during 1989–1999, 1999–2007, and 2007–2025 (**c**).

3.3.2. Changes in Sediment Erosion and Deposition at 8–14 m

From 1989 to 2025, the sediment deposition within the 8–14 m water level range of Poyang Lake generally exhibited a phased trend of "deposition-erosion-deposition," with a total net deposition of 3018.6 × 10^4 t over the entire period. Specifically, from 1989 to 1999, this water level range was dominated by deposition, with a deposition volume of 1092.0 × 10^4 t and an annual deposition rate of 109.2 × 10^4 t/a. From 1999 to 2007, the lake basin shifted to erosion, with an erosion volume of 2052.0 × 10^4 t and an annual erosion rate of 256.5 × 10^4 t/a. From 2007 to 2025, the lake basin shifted back to deposition, with a deposition volume of 3984.0 × 10^4 t and an annual deposition rate of 221.3 × 10^4 t/a (Figure 7).

Uncertainty in the VCM estimates arises mainly from water-area extraction (±3.54% relative to visual interpretation), the quadratic water level–area fitting (relative SEE < 10%), water-level reading errors and the bulk-density assumption. Propagating the first two terms, which dominate, yields a relative uncertainty of roughly 10–15% for the 8–14 m volume and sediment-mass estimates. Therefore, this uncertainty is negligible for lake volume change in each phase. What is more, the value is consistent with the independent gauge-based sediment budgets (Section 4.1), supporting the reliability of the phased pattern.

4. Discussion

4.1. Impact of Sediment Changes on Poyang Lake Evolution

As a river-connected shallow-water lake, the erosion and deposition of the Poyang Lake basin are controlled by sediment input and output [49]. From 1989 to 1999, the Poyang Lake basin experienced a pluvial period; increased precipitation led to enhanced soil erosion intensity within the basin and a rise in sediment concentration flowing into the lake [36,50]. Statistical data also indicated that from 1989 to 1999, sediment input from the Five Rivers exceeded sediment output at Hukou, Poyang Lake, resulting in a net sediment deposition of 4568.6 × 10^4 t (Figure 8). Since the beginning of the 21st century, a large number of reservoirs and water conservancy projects have been constructed in the Poyang Lake basin. These projects have played a role in sediment trapping, reducing the sediment supply to the lake area [30]. From 2000 to 2016, sediment input from the Five Rivers was less than sediment output, resulting in a net sediment erosion of 10,189.9 × 10^4 t (Figure 8). Since 2016, although soil and water conservation projects in the basin have reduced the amount of sediment entering the lake to some extent, the sediment output of Poyang Lake has also decreased significantly [39]. Statistical data also showed that from 2017 to 2024, sediment input from the Five Rivers exceeded sediment output at Hukou, Poyang Lake, resulting in a net sediment deposition of 627.7 × 10^4 t (Figure 8).

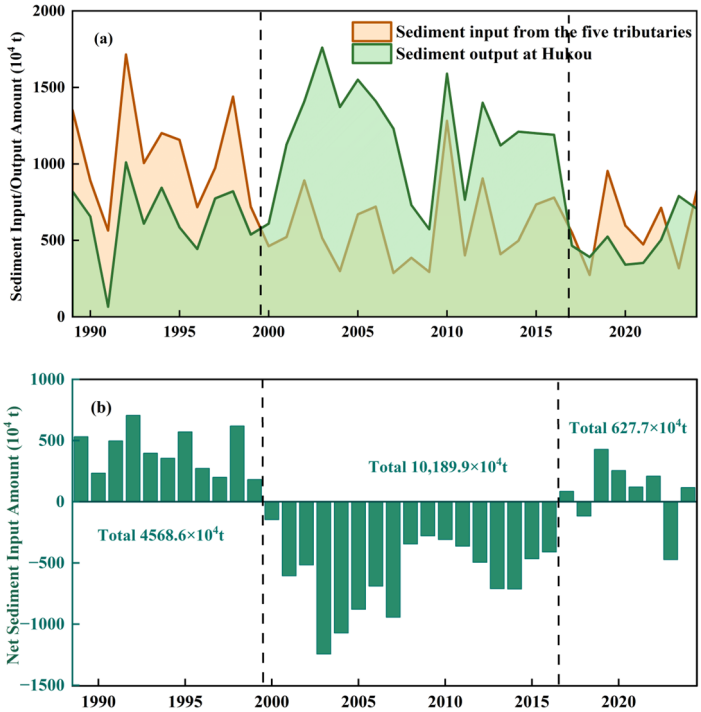


Figure 8. Interannual sediment inflow from the Five Rivers and outflow at Hukou (**a**); Net sediment inflow from the Five Rivers to Poyang Lake (**b**). Dashed lines denote the boundaries for stage division.

It should be noted that the gauge-based net sediment budgets (Figure 8) are considerably larger in magnitude than the erosion and deposition estimated by the VCM for the 8–14 m layer. For 1989–1999, the VCM-derived deposition (1092.0 × 10^4 t) accounts for about 24% of the gauge-based net deposition (4568.6 × 10^4 t). For the erosion phase, the VCM-derived erosion (2052.0 × 10^4 t during 1999–2007) is about 20% of the gauge-based net erosion during 2000–2016 (10189.9 × 10^4 t). Several factors account for this difference. First, the VCM quantifies only the 8–14 m layer, whereas the gauge budget integrates the whole lake. Second, the gauge budget is the difference between sediment input and output of the whole lake, whereas the VCM measures the net morphological change of the basin directly. Third, the statistical periods of the two approaches differ and the bulk density of 1.2 t/m^3 is an approximation. Thus, despite these quantitative differences, the two independent approaches consistently resolve the shift from deposition to erosion around 2000 and the return to deposition in the most recent period, which strengthens the credibility of the results.

4.2. Impact of Sand Mining Regulation on Poyang Lake Morphodynamics

Before 2000, the Poyang Lake basin within the 8–14 m water level range was in a state of deposition. During 1999–2007, however, the basin in this interval shifted to erosion (Figure 7b), with a total erosion of 2052.0 × 10^4 t (Figure 7c). This shift was closely associated with the adjustment of sand-mining policies (Section 2.3.1): after sand mining was prohibited in the main stem of the Yangtze River in 2000, a large number of sand-mining vessels moved into Poyang Lake [37,43]. Sand-mining operations mainly took place near the dry-season lake basin, leaving obvious mining traces in that part of the basin (Figure 9). High-resolution bathymetric and sub-bottom profiling has further shown that mining-induced incision of the channels propagated into the adjacent bottomlands [35], which explains why the volume of the entire 8–14 m layer, and not only that of the mined channels, increased during this period. With the stepwise tightening of sand-mining regulation after 2008 and the promulgation of the Regulations on the Administration of River Sand Mining in Jiangxi Province in 2016 (Section 2.3.1), in-lake sand extraction was greatly reduced; the 8–14 m layer shifted back to deposition after 2007, with a total deposition of 3984.0 × 10^4 t (Figure 7c). This indicates that policy regulation influenced the changes in Poyang Lake basin volume by controlling sand-mining intensity [43,51].

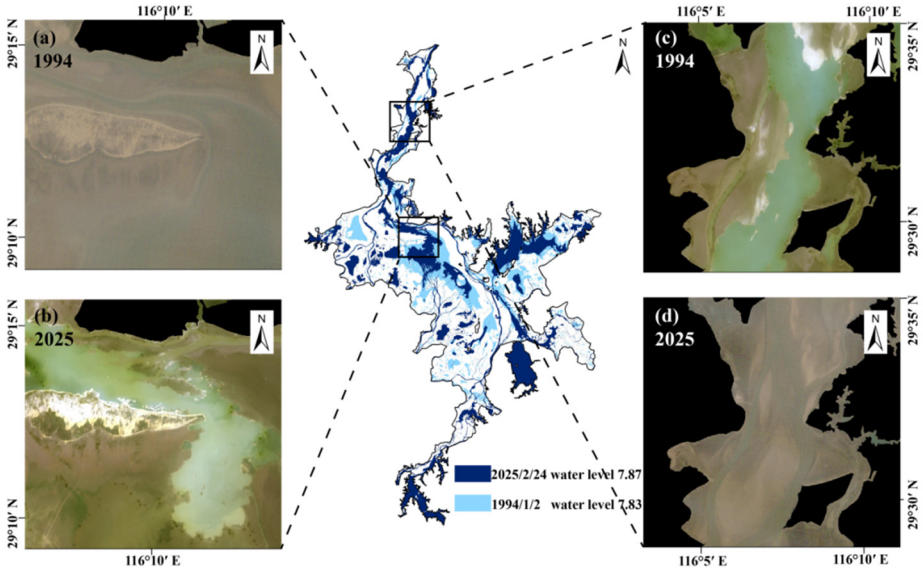


Figure 9. Site-specific lake basin alterations induced by sand mining. (**a**,**b**) Alterations in the central area of Poyang Lake. (**c**,**d**) Alterations at the lake-river passage area of Poyang Lake.

Previous studies have suggested that other engineering projects, besides sand mining, may also cause changes in the Poyang Lake basin [52]. For instance, the impoundment of the Three Gorges Project in the upper Yangtze River has weakened the backwater effect of the Yangtze River, leading to enhanced sediment transport capacity in the Hukou reach and consequent changes in the lake basin volume [40].

4.3. Implications and Limitations

The eco-hydrological environments of most lakes worldwide have experienced significant changes due to natural and anthropogenic disturbances [1,10]. Previous studies of Poyang Lake have quantified long-term lake dynamics [21], estimated lake water storage [18–20], and investigated the hydrological consequences of bathymetric change [22,23]. Satellite-based evidence of erosion and deposition within the lake has also been reported [15]. Based on these studies, the VCM converts area changes at fixed water levels directly into basin-volume and sediment-mass changes. We found that Poyang Lake volume (8–14 m) decreased by 2515.5×10^4 m^3 over 1989–2025, with deposition (1092.0×10^4 t), erosion (2052.0×10^4 t) and renewed deposition (3984.0×10^4 t) during 1989–1999, 1999–2007 and 2007–2025, respectively (Figure 7). The erosion phase identified here coincides with the period of intensive sand mining documented by Qi et al. [14], Lai et al. [16] and Zhang et al. [15]. The VCM offers a replicable method for limnological and geomorphological studies of other shallow-water lakes lacking long-term bathymetric data. The "deposition–erosion–deposition" pattern of Poyang Lake from 1989 to 2025 reflects the coupled influences of precipitation, sediment transport and sand-mining regulation, providing a scientific basis for sustainable water-resource management, ecological water-level management, flood and drought mitigation, and wetland conservation.

Nevertheless, this study focuses on the 8–14 m layer and covers neither the main channels below 8 m, where intensive sand mining occurred, nor the floodplains above 14 m. The results therefore describe the bottomland-dominated part of the basin rather than the whole lake. The accuracy validation of water extraction relied on a limited number of scenes, and the propagated uncertainty of the volume estimates is on the order of 10–15% (Section 3.3.2). Thus, independent validation against published bathymetric DEMs or official stage–storage curves is needed in future work.

5. Conclusions

This study constructed a volume change model (VCM) to estimate changes in shallow-water lakes. As an example, the Poyang Lake water storage (volume) across water levels ranging from 8 m to 14 m during 1989–2025 was calculated. The main conclusions are as follows:

(1) The constructed volume change model can effectively quantify the morphological evolution of shallow-water lakes. By comparing surface water areas at fixed water levels (8 m and 14 m), the VCM provides a replicable approach for shallow-water lakes lacking long-term bathymetric data.

(2) From 1989 to 2025, the volume of the Poyang Lake basin decreased by 2515.5×10^4 m^3, corresponding to a net sediment deposition of 3018.6×10^4 t.

(3) The evolution of sediment erosion and deposition in Poyang Lake is closely associated with the combined effects of watershed sediment changes, sand mining policy regulation, and human engineering activities. These findings provide scientific support for sustainable sand-mining regulation, ecological water-level management and wetland conservation in Poyang Lake and other river-connected shallow-water lakes.

Author Contributions: Conceptualization, Y.L. and S.Z.; methodology, Y.L. and S.Z.; software, Y.X. and L.L.; validation, J.F., J.Z. and L.L.; formal analysis, Z.L. and J.F.; investigation, Y.X., Z.L. and J.Z.; data curation, L.L. and J.Z.; writing—original draft preparation, Y.L., L.L. and S.Z.; writing—review and editing, Y.X., Z.L. and S.Z.; funding acquisition, J.F., Z.L. and S.Z. All authors have read and agreed to the published version of the manuscript.

Funding: This research was funded by the Natural Science Foundation of Shandong Province, grant numbers ZR2026MS0580 and ZR2025MS539.

Institutional Review Board Statement: Not applicable.

Informed Consent Statement: Not applicable.

Data Availability Statement: The Landsat Collection 2 Level-2 surface reflectance images are publicly available through the Google Earth Engine platform (https://code.earthengine.google.com (accessed on 22 July 2025)); the hydrological data are available from the Changjiang Water Resources Commission of the Ministry of Water Resources (http://www.cjw.gov.cn accessed on 4 June 2026); and the GEE scripts used in this study are available from the corresponding author upon reasonable request.

Conflicts of Interest: The authors declare no conflicts of interest.

References

1. Yao, F.; Livneh, B.; Rajagopalan, B.; Wang, J.; Crétaux, J.; Wada, Y.; Bergé-Nguyen, M. Satellites reveal widespread decline in global lake water storage. *Science* **2023**, *380*, 743–749. [CrossRef] [PubMed]
2. Xu, F.; Zhang, G.; Woolway, R.I.; Yang, K.; Wada, Y.; Wang, J.; Crétaux, J.F. Widespread societal and ecological impacts from projected Tibetan Plateau lake expansion. *Nat. Geosci.* **2024**, *17*, 516–523. [CrossRef]
3. Hutchinson, G.E.; Edmondson, Y.H. *A Treatise on Limnology*; John Wiley & Sons: New York, NY, USA, 1957; Volume 59, pp. 169–176.
4. Williamson, C.E.; Saros, J.E.; Vincent, W.F.; Smol, J.P. Lakes and reservoirs as sentinels, integrators, and regulators of climate change. *Limnol. Oceanogr.* **2009**, *54*, 2273–2282. [CrossRef]
5. Liu, H.; Zeng, W.; Lai, Z.; He, M.; Lin, C.; Ouyang, W.; Liu, X. Comparison of antimony and arsenic behaviour at the river-lake junction in the middle of the Yangtze River Basin. *J. Environ. Sci.* **2024**, *136*, 189–200. [CrossRef] [PubMed]
6. Guo, W.; Yang, J.; Yu, Z.; Lan, J.; Wang, H. Water Level Variation in Poyang Lake: Characteristics and Research on Suitable Ecological Water Level. *J. Oceanol. Limnol.* **2026**, *53*, 683–693. [CrossRef]
7. Li, T.; Liao, Q.; Wang, S.; Fu, B. Divergent change patterns observed in hydrological fluxes entering China's two largest lakes. *Sci. Total Environ.* **2022**, *817*, 152969. [CrossRef] [PubMed]
8. Scheffer, M. *Ecology of Shallow Lakes*; Kluwer Academic Publishers: Dordrecht, The Netherlands, 2004.
9. Mason, I.M.; Guzkowska, M.A.J.; Rapley, C.G.; Street-Perrott, F.A. The response of lake levels and areas to climatic change. *Clim. Change* **1994**, *27*, 161–197. [CrossRef]
10. Zhao, G.; Gao, H.; Li, Y.; Tang, Q.; Woolway, R.I.; Merder, J.; Rosa, L.; Michalak, A.M. Decoupling of surface water storage from precipitation in global drylands due to anthropogenic activity. *Nat. Water* **2025**, *3*, 80–88. [CrossRef]
11. Zhao, G.; Li, Y.; Zhou, L.; Gao, H. Evaporative water loss of 1.42 million global lakes. *Nat. Commun.* **2022**, *13*, 3686. [CrossRef] [PubMed]
12. Barnett, T.P.; Pierce, D.W. When will Lake Mead go dry? *Water Res. Res.* **2008**, *44*, 258–260. [CrossRef]
13. Woolway, R.I.; Kraemer, B.M.; Lenters, J.D.; Merchant, C.J.; O'Reilly, C.M.; Sharma, S. Global lake responses to climate change. *Nat. Rev. Earth Environ.* **2020**, *1*, 388–403. [CrossRef]
14. Qi, S.; Zhang, X.; Wang, D.; Zhu, J.; Fang, C. Study of morphologic change in Poyang Lake basin caused by sand dredging using multi-temporal Landsat images and DEMs. *Int. Arch. Photogramm. Remote Sens. Spat. Inf. Sci.* **2014**, *40*, 355–362. [CrossRef]
15. Zhang, S.; Liu, Y.; Yang, Y.; Sun, C.; Li, F. Erosion and deposition within Poyang Lake: Evidence from a decade of satellite data. *J. Gt. Lakes Res.* **2016**, *42*, 364–374. [CrossRef]
16. Lai, X.; Shankman, D.; Huber, C.; Yesou, H.; Huang, Q.; Jiang, J. Sand mining and increasing Poyang Lake's discharge ability: A reassessment of causes for lake decline in China. *J. Hydrol.* **2014**, *519*, 1698–1706. [CrossRef]
17. Pan, F.; Xi, X.; Wang, C. A comparative study of water indices and image classification algorithms for mapping inland surface water bodies using Landsat imagery. *Remote Sens.* **2020**, *12*, 1611. [CrossRef]
18. Tan, Z.; Melack, J.; Li, Y.; Liu, X.; Chen, B.; Zhang, Q. Estimation of water volume in ungauged, dynamic floodplain lakes. *Environ. Res. Lett.* **2020**, *15*, 054021. [CrossRef]

19. Xu, Y.; Li, J.; Wang, J.; Chen, J.; Liu, Y.; Ni, S.; Zhang, Z.; Ke, C. Assessing water storage changes of Lake Poyang from multi-mission satellite data and hydrological models. *J. Hydrol.* **2020**, *590*, 125229. [CrossRef]
20. Wang, F.; Zhou, Q.; Gao, H.; Wen, Y.; Zhou, S. Dynamic monitoring of Poyang Lake water area and storage changes from 2002 to 2022 via remote sensing and satellite gravimetry techniques. *Remote Sens.* **2024**, *16*, 2408. [CrossRef]
21. Qiu, H.; Zhang, Q. Analysis of spatiotemporal change characteristics of Poyang Lake from 1984 to 2021 based on GEE. *Sci. Rep.* **2025**, *15*, 41594. [CrossRef] [PubMed]
22. Zhang, Q.; Ye, X.C.; Werner, A.D.; Li, Y.L.; Yao, J.; Li, X.H.; Xu, C.Y. An investigation of enhanced recessions in Poyang Lake: Comparison of Yangtze River and local catchment impacts. *J. Hydrol.* **2014**, *517*, 425–434. [CrossRef]
23. Yao, J.; Zhang, Q.; Ye, X.; Zhang, D.; Bai, P. Quantifying the impact of bathymetric changes on the hydrological regimes in a large floodplain lake: Poyang Lake. *J. Hydrol.* **2018**, *561*, 711–723. [CrossRef]
24. Feng, L.; Hu, C.; Chen, X.; Cai, X.; Tian, L.; Gan, W. Assessment of inundation changes of Poyang Lake using MODIS observations between 2000 and 2010. *Remote Sens. Environ.* **2012**, *121*, 80–92. [CrossRef]
25. Li, Y.; Tan, Z.; Zhang, Q.; Liu, X.; Chen, J.; Yao, J. Refining the concept of hydrological connectivity for large floodplain systems: Framework and implications for eco-environmental assessments. *Water Res.* **2021**, *195*, 117005. [CrossRef] [PubMed]
26. Song, Z.; Zhu, G.; Zhu, M.; Xu, H.; Cai, Y.; Zhang, Y.; Gui, Z.; Zou, W.; Fan, Z. Limiting factors on aquatic ecological health of Caizi Lake, a Changjiang River-isolated shallow lake: Implications for lake restoration. *J. Oceanol. Limnol.* **2025**, *43*, 1923–1937. [CrossRef]
27. Mei, X.; Dai, Z.; Fagherazzi, S.; Chen, J. Dramatic variations in emergent wetland area in China's largest freshwater lake, Poyang Lake. *Adv. Water Res.* **2016**, *96*, 1–10. [CrossRef]
28. Wang, H.; Zhang, L.; Yao, X.; Xue, B.; Yan, W. Dissolved nitrous oxide and emission relating to denitrification across the Poyang Lake aquatic continuum. *J. Environ. Sci.* **2017**, *52*, 130–140. [CrossRef] [PubMed]
29. Yao, J.; Zhang, Q.; Li, Y.; Li, M. Hydrological evidence and causes of seasonal low water levels in a large river-lake system: Poyang Lake, China. *Hydrol. Res.* **2016**, *47*, 24–39. [CrossRef]
30. Lai, G.; Wang, P.; Li, L. Possible impacts of the Poyang Lake (China) hydraulic project on lake hydrology and hydrodynamics. *Hydrol. Res.* **2016**, *47*, 187–205. [CrossRef]
31. Dade, W.B. Grain size, sediment transport and alluvial channel pattern. *Geomorphology* **2000**, *35*, 119–126. [CrossRef]
32. Jiang, F.; Qi, S.; Liao, F.; Ding, M.; Wang, Y. Vulnerability of Siberian crane habitat to water level in Poyang Lake wetland, China. *GISci. Remote Sens.* **2014**, *51*, 662–676. [CrossRef]
33. Luo, W.; Han, Y.; Yan, L.; Xia, J.; Tang, G. Hydromorphological adjustment and river–lake disconnection in the Jingjiang Reach under long-term regulation of three Gorges Reservoir. *Geomorphology* **2025**, *495*, 110113. [CrossRef]
34. Guo, H.; Hu, Q.; Zhang, Q.; Feng, S. Effects of the three gorges dam on Yangtze river flow and river interaction with Poyang Lake, China: 2003–2008. *J. Hydrol.* **2012**, *416*, 19–27. [CrossRef]
35. Zheng, S.; Cheng, H.; Tang, M.; Xu, W.; Liu, E.; Gao, S.; Best, J.; Jiang, Y.; Zhou, Q. Sand mining impact on Poyang Lake: A case study based on high-resolution bathymetry and sub-bottom data. *J. Oceanol. Limnol.* **2022**, *40*, 1404–1416. [CrossRef]
36. Zhang, Q.; Sun, P.; Chen, X.; Jiang, T. Hydrological extremes in the Poyang Lake basin, China: Changing properties, causes and impacts. *Hydrol. Process.* **2011**, *25*, 3121–3130. [CrossRef]
37. Wu, G.; Cui, L.J. Remote sense-based analysis of sand dredging impact on water clarity in Poyang Lake. *Acta Ecol. Sin.* **2008**, *28*, 6113–6120.
38. Leeuw, J.D.; Shankman, D.; Wu, G.; Boer, W.F.D.; Burnham, J.; He, Q.; Yesou, H.; Xiao, R. Strategic assessment of the magnitude and impacts of sand mining in Poyang Lake, China. *Reg. Environ. Change* **2010**, *10*, 95–102. [CrossRef]
39. Gu, C.; Mu, X.; Gao, P.; Zhao, G.; Sun, W.; Li, P. Effects of climate change and human activities on runoff and sediment inputs of the largest freshwater lake in China, Poyang Lake. *Hydrol. Sci. J.* **2017**, *62*, 2313–2330. [CrossRef]
40. Liu, Y.; Wu, G. Hydroclimatological influences on recently increased droughts in China's largest freshwater lake. *Hydrol. Earth Syst. Sci.* **2016**, *20*, 93–107. [CrossRef]
41. Changjiang Water Resources Commission of the Ministry of Water Resources. Available online: http://www.cjw.gov.cn/ (accessed on 4 June 2026).
42. General Office of the State Council of China. Notice on Opinions for Strengthening Sand Mining Administration in the Middle and Lower Reaches of the Yangtze River. Available online: https://www.gov.cn/gongbao (accessed on 12 June 2026).
43. Li, J.; Tian, L.; Chen, X.; Li, X.; Huang, J.; Lu, J.; Feng, L. Remote-sensing monitoring for spatio-temporal dynamics of sand dredging activities at Poyang Lake in China. *Int. J. Remote Sens.* **2014**, *35*, 6004–6022. [CrossRef]
44. Jiangxi Provincial People's Government. Regulations on River Channel Sand Mining Management in Jiangxi Province. Available online: http://ncx.nc.gov.cn (accessed on 8 June 2026).
45. Xu, H. Modification of normalised difference water index (NDWI) to enhance open water features in remotely sensed imagery. *Int. J. Remote Sens.* **2006**, *27*, 3025–3033. [CrossRef]
46. Otsu, N. A threshold selection method from gray-level histograms. *IEEE Trans. Syst. Man Cybern.* **1979**, *9*, 62–66. [CrossRef]

47. Cordeiro, M.C.; Martinez, J.M.; Peña-Luque, S. Automatic water detection from multidimensional hierarchical clustering for Sentinel-2 images and a comparison with Level 2A processors. *Remote Sens. Environ.* **2021**, *253*, 112209. [CrossRef]
48. Wang, J.; Dai, Z.; Mei, X.; Lou, Y.; Wei, W.; Ge, Z. Immediately downstream effects of Three Gorges Dam on channel sandbars morphodynamics between Yichang-Chenglingji Reach of the Changjiang River, China. *J. Geogr. Sci.* **2018**, *28*, 629–646. [CrossRef]
49. Gautier, E.; Brunstein, D.; Vauchel, P.; Jouanneau, J.; Roulet, M.; Garcia, C.; Guyot, J.; Castro, M. Channel and floodplain sediment dynamics in a reach of the tropical meandering Rio Beni (Bolivian Amazonia). *Earth Surf. Process. Landf.* **2010**, *35*, 1838–1853. [CrossRef]
50. Zhao, B.; Wu, J.; Tian, F.; Liu, M.; Chen, M.; Lin, J. Temporal and Spatial changes in flood disaster risk over the past 30 years in the Poyang lake region, China. *Nat. Hazards* **2025**, *121*, 12487–12515. [CrossRef]
51. Duan, H.; Cao, Z.; Shen, M.; Liu, D.; Xiao, Q. Detection of illicit sand mining and the associated environmental effects in China's fourth largest freshwater lake using daytime and nighttime satellite images. *Sci. Total Environ.* **2019**, *647*, 606–618. [CrossRef] [PubMed]
52. Hu, B.; Yang, Z.; Wang, H.; Sun, X.; Bi, N.; Li, G. Sedimentation in the Three Gorges Dam and the future trend of Changjiang (Yangtze River) sediment flux to the sea. *Hydrol. Earth Syst. Sci.* **2009**, *13*, 2253–2264. [CrossRef]

Disclaimer/Publisher's Note: The statements, opinions and data contained in all publications are solely those of the individual author(s) and contributor(s) and not of MDPI and/or the editor(s). MDPI and/or the editor(s) disclaim responsibility for any injury to people or property resulting from any ideas, methods, instructions or products referred to in the content.